

From depth-averaging to fully three-dimensional modelling of debris-flow dynamics

*Original*

From depth-averaging to fully three-dimensional modelling of debris-flow dynamics / Pirulli, M.; Leonardi, A.; Manassero, M.; Scavia, C.. - ELETTRONICO. - (2019), pp. 1-7. ( 17th European Conference on Soil Mechanics and Geotechnical Engineering, ECSMGE 2019 Reykjavik, Iceland 1-6 September 2019) [10.32075/17ECSMGE-2019-1084].

*Availability:*

This version is available at: 11583/2972084 since: 2022-10-05T09:53:16Z

*Publisher:*

ISSMGE

*Published*

DOI:10.32075/17ECSMGE-2019-1084

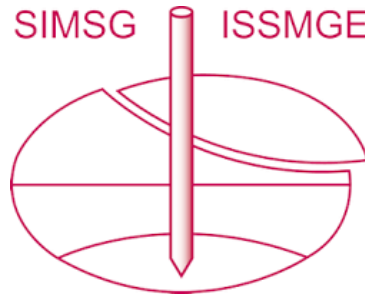
*Terms of use:*

This article is made available under terms and conditions as specified in the corresponding bibliographic description in the repository

*Publisher copyright*

(Article begins on next page)

# INTERNATIONAL SOCIETY FOR SOIL MECHANICS AND GEOTECHNICAL ENGINEERING



*This paper was downloaded from the Online Library of the International Society for Soil Mechanics and Geotechnical Engineering (ISSMGE). The library is available here:*

<https://www.issmge.org/publications/online-library>

*This is an open-access database that archives thousands of papers published under the Auspices of the ISSMGE and maintained by the Innovation and Development Committee of ISSMGE.*

# From depth-averaging to fully three-dimensional modelling of debris-flow dynamics

## Dynamique des laves torrentielles: depuis la modelisation type depth-averaged à la modelisation tridimensionnelle

M. Pirulli

*Politecnico di Torino, Torino, Italy*

A. Leonardi, M. Manassero, C. Scavia

*Politecnico di Torino, Torino, Italy*

**ABSTRACT:** Two numerical codes, with fundamental differences in their approaches, are used for modeling the Yu Tung debris flow, which occurred in Hong Kong in 2008. The first code, RASH3D, is based depth-averaged St. Venant equations, solved in an Eulerian framework. The second code, HYBIRD, is fully 3D and based on Lattice-Boltzmann Model (LBM), i.e. the conservation equations are not depth-averaged and therefore multiple velocity measures are available over the depth. The two model output are compared and discussed.

**RÉSUMÉ:** Deux codes numériques, aux approches différentes, sont utilisés pour modéliser la lave torrentielle survenue à Yu Tung (Hong Kong) en 2008. Le premier code, RASH3D, est basé sur des équations de St. Venant à moyenne de profondeur, résolues dans un cadre Eulérien. Le deuxième code, HYBIRD, est entièrement 3D et basé sur le modèle de Lattice-Boltzmann (LBM), c'est-à-dire que les équations de conservation ne sont pas moyennées en profondeur et que, par conséquent, de multiples mesures de vitesse sont disponibles sur la profondeur. Les résultats des deux modèles sont comparés et discutés.

**Keywords:** debris flow; numerical modelling; continuum mechanics; back analysis

## 1 INTRODUCTION

Debris flows are gravity-driven, highly concentrated mixtures of sediment and water commonly composed of poorly sorted rock, soil, organic matter, and sundry debris (Major, 1997).

In alpine areas, they are one of the most devastating landslide phenomena, in terms of loss of life and damages to structures and infrastructures. Their destructive potential is due to the absence of premonitory signs, the extremely high velocity (0.05-20 m/s), the

erosive capability and the long travel distance also on low-inclination slopes.

Predicting the evolution (e.g. velocity, run-out distance, deposit final shape) of these phenomena through numerical modeling can contribute to develop more precise hazard maps, and design more effective countermeasure.

This paper presents two methods, both implemented in in-house codes, that are different on various theoretical and practical aspects. The first method, implemented in the code RASH3D (Pirulli, 2005, Pirulli et al., 2007), solves a depth-averaged version of the Navier-Stokes equations.

The second, implemented in the code HYBIRD (Leonardi et al., 2016), is based on the Lattice-Boltzmann Method (LBM) and, rather than solving the Navier-Stokes equation directly, performs a solution of the Boltzmann equation. More details about the numerical methods are given in the next sections. However, a key difference in the two approaches consists in the following: RASH3D is based on a standard depth-averaging technique, where the topography is implemented using (x,y,z) points, but only a single value for depth-averaged quantities (height, velocity, shear rate, basal stress) is stored for each (x,y) point in the computational grid. This greatly boost the performance of the code. In this respect, the apex “3D” only refers to the capability of the code to read and solve 3D topographies. In HYBIRD, on the other hand, local values for velocity, pressure and shear rate are obtained for each fluid point in (x,y,z). This requires a larger allocation of resources, and much longer computational times. However, the model requires no assumption on the shape of the velocity profile, and allows to directly implement rheological laws, returning a complete 3D velocity field.

After a short description of the two models, the codes are used to back analyse the debris flow that occurred in 2008 in Hong Kong. The obtained results are presented and discussed.

## 2 RASH3D

The numerical code RASH3D is based on a one-phase continuum mechanics approach, and on depth-averaged St. Venant equations. The real heterogeneous mass is replaced with an incompressible equivalent fluid, whose behaviour is described by the depth-averaged balance equations of mass and momentum:

$$\left\{ \begin{array}{l} \frac{\partial h}{\partial t} + \frac{\partial(v_x h)}{\partial x} + \frac{\partial(v_y h)}{\partial y} = 0 \\ \frac{\partial h v_x}{\partial t} + \frac{\partial h v_x^2}{\partial x} + \frac{\partial v_x v_y}{\partial y} = \frac{\partial(g_z h^2/2)}{\partial x} + \frac{1}{\rho} \tau_{zx} + g_x h \\ \frac{\partial h v_y}{\partial t} + \frac{\partial v_x v_y}{\partial x} + \frac{\partial h v_y^2}{\partial y} = \frac{\partial(g_z h^2/2)}{\partial y} + \frac{1}{\rho} \tau_{zy} + g_y h \end{array} \right. \quad (1)$$

where:

- $v_x, v_y$  denote the depth-averaged flow velocities in the x and y directions (z is normal to the topography);
- h is the flow depth;
- $\tau_{zx}, \tau_{zy}$  are the shear resistance stresses;
- $\rho$  is the mass density
- $g_x, g_y, g_z$  are the projections of the gravity vector in the x-, y-, z- directions, respectively.

The governing equations (1) are solved in RASH3D using an Eulerian framework, on a triangular finite element mesh, through a kinetic scheme that is based on a finite volume (Mangeney-Castelnau et al. 2003).

### 2.1 Rheological laws

The rheology of the material is modelled by a single term, which describes the basal shear stress that develops at the interface between the moving mass and the sliding surface. A geographic information system (GIS) integrated function makes it possible to change the type of rheology and/or the rheological parameter values along the run-out path to allow changes to be made to the flow characteristics during flow propagation (Pirulli et al., 2017).

The following relationships are implemented in RASH3D:

- Frictional rheology, the resisting shear forces at the base of the flowing mass are assumed to depend on the normal stress, but not on velocity

$$\tau_{zi} = -(\rho g h \tan \varphi) \frac{v_i}{\|v\|} \quad (2)$$

where  $\varphi$  is the dynamic basal friction angle;

- Turbulent rheology, which is characterized by intense mixing, at relatively high inertial to viscous stress ratios. The turbulent basal shear resistance is proportional to the square of the depth-averaged flow velocity, and it can be calculated using the Manning equation:

$$\tau_{zi} = -\left(\frac{\rho g n^2 h v_i^2}{h^{1/3}}\right) \frac{v_i}{\|v\|} \quad (3)$$

where  $n$  is the Manning roughness coefficient, and the subscript  $i = x, y$ , respectively.

One disadvantage of this approach is that it cannot reproduce the cessation of motion on gently sloping surfaces. Nevertheless, Costa (1997) and Jin and Fread (1999) showed that the flow depth and the velocity of a channelized flowing mass can be simulated reasonably well after calibration with Manning coefficient;

- Voellmy rheology, where the turbulent rheology disadvantage can be overcome by adding a frictional term in the rheological formulation that describes the stopping of the flow on a sloping surface (e.g. Hungr and McDougall 2009, Naef et al. 2006, Rickenmann et al. 2006). It results

$$\tau_{zi} = -\left(\rho g h \tan \varphi + \frac{\rho g v_i^2}{\xi}\right) \frac{v_i}{\|v\|} \quad (4)$$

which consists of a turbulent term,  $\xi$  that accounts for velocity-dependent friction losses, and a Coulomb or basal friction term,  $(\tan \varphi)$ , which is used to describe the stopping mechanism, where the basal friction angle  $\varphi$  is generally only a fraction of the Coulomb angle;

- Bingham rheology, which combines plastic and viscous behaviors. A so-called Bingham fluid behaves like a rigid material below a given threshold yield strength, but like a viscous material above this threshold. The basal shear resistance can be determined by solving the following cubic equation:

$$\tau_{zi}^3 + 3\left(\frac{\tau_0}{2} + \frac{\nu_B v_i}{h}\right) \tau_{zi}^2 - \frac{\tau_0^3}{2} = 0 \quad (5)$$

where  $\tau_0$  is the Bingham yield stress and  $\nu_0$  is the Bingham viscosity. The third-order polynomial has been solved and implemented in RASH3D using the polynomial economization technique proposed by Pastor et al. (2004);

- Quadratic rheology, in which the shear resistance stress is provided by the following expression:

$$\tau_{zi} = -\left(\tau_0 + \frac{k\nu_0}{8h} |v_i| + \rho g \frac{n_{td}^2 v_i^2}{h^{\frac{1}{3}}}\right) \frac{v_i}{\|v\|} \quad (6)$$

where  $n_{td}$  is the equivalent Manning coefficient for turbulent and dispersive shear stress components and  $k$  is the flow resistance parameter (O'Brien et al. 1993).

### 3 HYBIRD

HYBIRD is a code originally conceived as a combination of the Discrete Element Method (DEM) and LBM (Leonardi et al., 2014; Leonardi et al., 2015). This work sees the first application of the code at the full topographical scale. Therefore, to limit the number of unknowns, only the LBM part of the code is tested.

HYBIRD utilizes concepts from the kinetic theory, and discretizes an Eulerian probability density function (pdf)  $f(\mathbf{x}, \mathbf{c}, t)$ , which indicates the probability of finding a fluid particle with microscopic velocity  $\mathbf{c}$  at position  $\mathbf{x}$  and time  $t$ . In addition to the usual discretization in the time- and space domains, also the velocity space is discretized by selecting only a finite set of allowed microscopic velocities  $\mathbf{c}_i$ . Thus, the discretized form of the pdf reads  $f_i(\mathbf{x}, t) = f(\mathbf{x}, \mathbf{c}_i, t)$ . The standard macroscopic velocity and density fields are then reconstructed by simple summation at every node:

$$\begin{cases} \rho(\mathbf{x}, t) = \sum_i f_i(\mathbf{x}, t) \\ \mathbf{v}(\mathbf{x}, t) = \sum_i f_i(\mathbf{x}, t) \mathbf{c}_i / \rho(\mathbf{x}, t) \end{cases} \quad (7)$$

The evolution of the pdf is controlled by the Boltzmann equation:

$$\frac{df}{dt} = \Omega_{coll} \quad (8)$$

where  $\Omega_{coll}$  is the collision operator, implementing the effect of viscous dissipation. The time discretization is explicit. For the full formulation and the theoretical background, please refer to Chen & Doolen (1998). Note that the shear rate tensor  $\dot{\gamma}_{ij}$  can be computed locally directly from the pdf, and thus the calculus of no velocity gradient is required (Leonardi et al., 2014).

### 3.1 Rheological laws

As there is no depth-integration procedure, stresses are applied everywhere on the domain, and are controlled by the rheological model, which can be chosen among the following:

- Bingham rheology. Linear shear-thinning behavior, analogous to the one implemented in RASH3D

$$\tau_{ij} = \frac{\tau_0 \dot{\gamma}_{ij}}{|\dot{\gamma}|} + \nu_0 \dot{\gamma}_{ij} \quad (9)$$

- Turbulent rheology. A turbulent viscosity is computed according to the Smagorinsky-Lily model (Leonardi et al. 2011), with a constant subgrid turbulence constant  $C_s=0.16$ .

$$\tau_{ij} = \nu_0 \dot{\gamma}_{ij} + \rho \Delta x^2 C_s^2 |\dot{\gamma}| \dot{\gamma}_{ij} \quad (10)$$

- Frictional rheology with rate-dependent friction coefficient

$$\tau_{ij} = \frac{\mu(I) p \dot{\gamma}_{ij}}{|\dot{\gamma}|} \quad (11)$$

Here the friction coefficient  $\mu$  is chosen to be a function of the Inertial number, a dimensionless quantity locally defined as  $I = d|\dot{\gamma}|/\sqrt{p/\rho}$ , with  $d$  the grain diameter (Jop et al., 2006). The relationship  $\mu(I)$  contains the three empirical constants  $\Delta\mu$ ,  $\mu_0$ , and  $I_0$ . Note that if  $\Delta\mu = 0$  the model reduces to a simpler frictional model with constant coefficient.

- Voellmy rheology. It combines frictional properties and turbulent dissipation:

$$\tau_{ij} = \frac{\tan \varphi p \dot{\gamma}_{ij}}{|\dot{\gamma}|} + \rho d^2 |\dot{\gamma}| \dot{\gamma}_{ij} \quad (12)$$

The turbulent dissipation is mesh-independent and is controlled by a Bagnold-like collisional length scale, which can be assumed to be the grain diameter  $d$ .

One of the main difficulty of working outside the depth-averaged framework is the calibration of the rheological parameters. As those are usually back-calculated, and are not directly obtained from the physical properties of the material, there is no guarantee that the same parameters will yield similar results when transferred from RASH3D to HYBIRD.

## 4 2008 YU TUNG ROAD DEBRIS FLOW, HONG KONG

The Yu Tung debris flow was recorded in June 2008, when a mass of about 2350 m<sup>3</sup> detached from a hillslope and invaded a nearby road. There is rich documentation about the event (AECOM, 2012), with velocity estimations at various locations, as shown in Fig. 1.

Accordingly to previously calibrated case histories in Hong Kong and to specific analyses carried out for the 2008 Yu Tung Road debris flow by Tattersall et al. (2009) (Table 1), the RASH3D numerical back analyses were carried out using either a Frictional (Case1) or a Voellmy rheology (Case2) in the source area combined

with a Voellmy rheology along the runout channel for both the Case1 and Case2. In particular, the change of rheology or values of rheological parameters between the source and the runout channel was necessary to simulate observed deposition of about 300 m<sup>3</sup> of debris within the landslide source area.

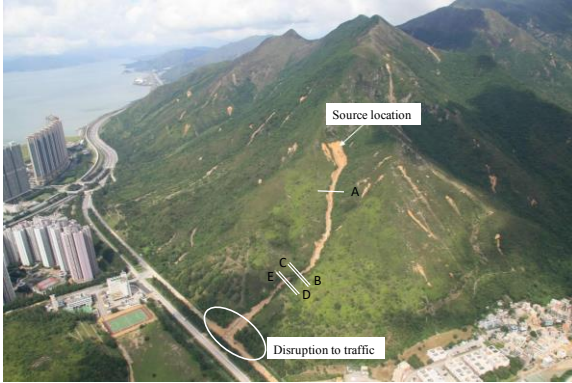


Figure 1. Yu Tung debris flow. The five sections indicate chainages (CH) where velocity estimates are available: A: CH100; B: CH413; C: CH439; D: CH462; E: CH477 (AECOM, 2012).

Starting from the Tatterstal et al. set of rheological values, RASH3D results are calibrated by trial-and-error to reproduce the flow dynamics in terms of on-site estimated velocities at the above mentioned chainages and capability of the simulated landslide debris to reach the road. The best fit rheological parameters for RASH3D are resumed in Table 1. The calibrated values are very close to those obtained by Tatterstal et al. (2009) with Debriflo, 2d-DMM and DAN3D.

Table 1. Yu Tung debris flow. Calibrated parameters for RASH3D

	Case 1	Case 2
<b>Source</b>	Frictional $\varphi=25^\circ$	Voellmy $\varphi=23^\circ, \xi=845\text{m/s}^2$
<b>Channel</b>	Voellmy $\varphi=8.5^\circ, \xi=750\text{m/s}^2$	Voellmy $\varphi=8.5^\circ, \xi=750\text{m/s}^2$

The Yu Tung debris flow is also back-analyzed using HYBIRD. In this case, the rheological

parameters used in precedent works and for RASH3D cannot be directly tested. However, some principles can be transferred, in particular the use of a Voellmy rheology, with a low angle of friction. In this case, the same rheology has been used consistently over the whole domain. Shear resistance is active in any direction, and at every location inside the 3D mass.

The comparison between field flow velocity along the talweg and numerical results for RASH3D (Case 1 and Case 2) and for HYBIRD (Case 3:  $\varphi=1.5^\circ, d=0.005\text{m}$ ) is shown in Figure 2. A rather good fit of velocities is observed for both models. The results evidence that, albeit substantial differences in the approach, RASH3D and HYBIRD give approximately the same values of flow velocities overall, and especially at chainages where the on-site flow velocity was estimated based on flow super-elevation. Note that for HYBIRD surface velocities are also available (i.e. not depth averaged). These are reported in the graph.

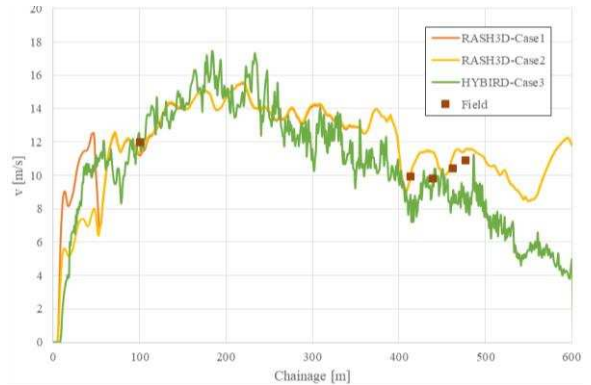


Figure 2. Yu Tung debris flow. Comparison between RASH3D and HYBIRD in terms of maximum flow speed (depth-averaged) and estimated velocities of the Yu Tung Debris Flow (brown squares).

As for the landslide debris spatial distribution during the runout process up to the final deposition, it is observed that for both models the whole mass reaches the road, see Figure 2. For RASH3D, since Case 1 better fits the deposition of debris in the source area, its representation in terms of flow process is given in the figure.

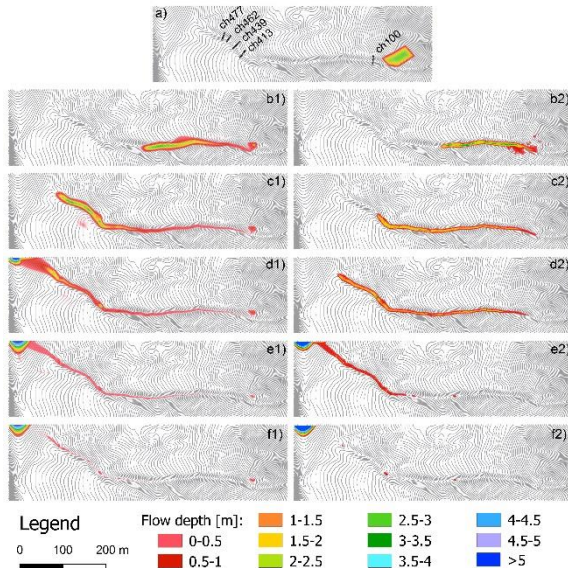


Figure 2. Yu Tung debris flow. Flow runout path, with flow-depth contours at different times: (a) 0 s, (b) 20 s, (c) 40 s, (d) 60 s, (e) 100 s, (f) 300 s. The left column shows the results obtained with RASH3D, the right column those obtained with HYBIRD.

## 5 CONCLUSIONS

In this work, we presented the numerical results obtained for the 2008 Yu Tung debris flow (Hong Kong) with RASH3D, a depth-averaged model, and also with HYBIRD, a full-3D code based on LBM which is still under development. A good comparison between the codes and with the field data have been obtained. The cross comparison carried out for Yu Tung represents one of the first attempt at moving beyond the depth-averaging paradigm. Once validated, HYBIRD can also be used to simulate structural countermeasures of arbitrary shape. Future studies will focus on this aspect.

## 6 ACKNOWLEDGEMENTS

Computational resources were provided by HPC@POLITO, a project of Academic Computing within the Department of Control and

Computer Engineering at Politecnico di Torino (<http://www.hpc.polito.it>)

## 7 REFERENCES

- AECOM. 2012. Detailed Study of the 7 June 2008 landslides on the hillside above Yu Tung Road, Tung Chung. *GEO Report* **271**, 124 p.
- Chen, S., & Doolen, G. D. 1998. Lattice Boltzmann Method for Fluid Flows. *Annual Review of Fluid Mechanics* **30**, 329–364.
- Costa, J.E. 1997. Hydraulic modeling for Lahar hazards at Cascades Volcanoes. *Environmental & Engineering Geoscience* **III(1)**, 21–30.
- Hung, O. & McDougall, S. 2009. Two numerical models for landslide dynamic analysis. *Computers & Geosciences* **35(5)**, 978–992.
- Jin, M. & Fread, D.L. 1999. 1D modeling of mud/debris unsteady flows. *J. Hydrol. Eng.* **125(8)**, 827–834.
- Jop, P., Forterre, Y., & Pouliquen, O. 2006. A constitutive law for dense granular flows. *Nature* **441(7094)**, 727–30.
- Leonardi, C. R., Owen, D. R. J., & Feng, Y. T. 2011. Numerical rheometry of bulk materials using a power law fluid and the lattice Boltzmann method. *Journal of Non-Newtonian Fluid Mechanics* **166(12–13)**, 628–638.
- Leonardi, A., Wittel, F. K., Mendoza, M., & Herrmann, H. J. 2014. Coupled DEM-LBM method for the free-surface simulation of heterogeneous suspensions. *Computational Particle Mechanics* **1**, 3–13.
- Leonardi, A., Cabrera, M., Wittel, F. K., Kaitna, R., Mendoza, M., Wu, W., & Herrmann, H. J. 2015. Granular-front formation in free-surface flow of concentrated suspensions. *Physical Review E - Statistical, Nonlinear, and Soft Matter Physics* **92(5)**, 052204.
- Leonardi, A., Wittel, F. K., Mendoza, M., Vetter, R., & Herrmann, H. J. 2016. Particle-Fluid-Structure Interaction for Debris Flow Impact

- on Flexible Barriers. *Computer-Aided Civil and Infrastructure Engineering* **31(5)**, 323–333.
- Major, J.J. 1997. Depositional processes in large-scale debris-flow experiments. *The Journal of Geology* **105**, 345-366.
- Mangeney-Castelnau, A., Vilotte, J.P., Bristeau, M.O., Perthame, B., Bouchut, F., Simeoni, C., Yerneni, S., 2003. Numerical modelling of avalanche based on Saint Venant equations using a kinetic scheme. *Journal of Geophysical Research* **108(B11)**.
- Naef, D., Rickenmann, D., Rutschmann, P. & McArdell, B. 2006. Comparison of flow resistance relations for debris flows using a one-dimensional finite element simulation model. *Natural Hazards and Earth System Science* **6**, 155-165.
- O'Brien, J.S., Julien, P.Y. & Fullerton, W.T. 1993. Two-dimensional water flood and mud flow simulation. *Journal of Hydraulic Engineering* **119(2)**, 244–261.
- Pastor, M., Quecedo, M., Gonzalez, E., Herreros, M.I., Fernandez Merodo, J.A. & Mira, P. 2004. Simple approximation to bottom friction for Bingham fluid depth integrated models. *Journal of Hydraulic Engineering* **130(2)**, 149-155.
- Pirulli, M. 2005. Numerical modelling of landslide runout, a continuum mechanics approach. *PhD Thesis*, Politecnico di Torino, Torino, Italy.
- Pirulli, M., Bristeau, M.O., Mangeney, A. & Scavia, C. 2007. The effect of the earth pressure coefficients on the runout of granular material. *Environmental Modelling & Software* **22(10)**, 1437-1454.
- Pirulli, M., Barbero, M., Marchelli, M. & Scavia, C. 2017. The failure of the Stava Valley tailings dams (Northern Italy): numerical analysis of the flow dynamics and rheological properties. *Geoenvironmental Disasters* **4(3)**, 1-15.
- Rickenmann, D., Laigle, D., McArdell, B. & Hubl, J. 2006. Comparison of 2D debris-flow simulation models with field events. *Computational Geosciences* **10**, 241-264.
- Tattersall, J.W., Devonald, D.M. & McDougall, S. 2009. Modelling of debris flows for the North Lantau Expressway and Tu Tung Road study area. *Proceedings, HKIE Geotechnical Division 29th Annual Seminar*, The Hong Kong Institution of Engineer, Geotechnical Division, 163-169.